Identification of the CH + O_2 → OH(A) + CO Reaction as the Source of OH(A−X) Chemiluminescence in C_2H_2/O/H/O_2 Atomic Flames and Determination of Its Absolute Rate Constant over the Range T = 296 to 511 K

S. A. Carl,* M. Van Poppel, and J. Peeters

Department of Chemistry, University of Leuven, Celestijnenlaan 200F, B-3001 Leuven, Belgium

Received: June 4, 2003; In Final Form: September 23, 2003

Optical and molecular beam sampling−threshold ionization mass-spectrometric (MB-TIMS) measurements have been applied to fast-flowing, low-pressure C_2H_2/O/H/O_2 reactive systems at temperatures in the range 296 to 511 K. At each temperature, the 308 nm OH(A→X) emission intensities were found to be directly proportional to the product of O_2 and CH concentrations, demonstrating that the CH + O_2 → OH(A) + CO reaction channel (1d) is the source of electronically excited hydroxyl radicals in C_2H_2/O/H/O_2 atomic flames. Calibration of the detection systems for [O_2], [CH], and [OH(A)] yields a room-temperature rate constant for the reaction channel CH + O_2 → OH(A) + CO of $k_{1d}(296\ \text{K}) = 8.0^{+10}_{-5} \times 10^{-14}$ cm^3 s^{-1}, while the determinations at higher temperatures give an activation energy for reaction 1d of $0.7^{+1.3}_{-0.7}$ kJ mol^{-1} over the 296 to 511 K range.

1. Introduction

The electronically excited species CH($A^2\Delta$, $B^2\Sigma^-$), OH($A^2\Sigma^+$), C_2($d^3\Pi_g$), HCO(A^2A'', B^2A'), CO($A^1\Pi$, $d^3\Delta$, $a^3\Pi$), which are thought to arise from only a small number of highly exothermic reactions, are responsible for nearly all banded emissions of hydrocarbon flames in the visible and near UV.[1−8] Under most circumstances these electronically excited species are of little consequence to the chemical environment, as their concentrations are extremely low due to their low production rates, through minor product channels, and rapid removal rates by radiative decay and collisional quenching. The fast removal also provides the important feature that they are in quasi-steady-state, so that their photon emission rate provides information on the concentration product of their precursors. Furthermore, this information can be highly spatially and temporally resolved because the removal rates of the precursor species due to chemical reaction and molecular transport mechanisms are much lower than those of the electronically excited species.

Detailed spectroscopic information and physical quenching data have long been available for most of the above-mentioned electronically excited species. However, meaningful interpretation of flame chemiluminescence measurements[9] in terms of the underlying chemistry requires knowledge at least of the reaction, or reactions, leading to formation of the electronically excited species. Direct experimental evidence on which reaction, of sometimes several candidate reactions, is responsible for the production of the electronically excited species is scarce, and only recently has such data been published.[5] Once identified though, an obstacle to quantitative interpretation remains the determination of the pertinent absolute rate constant.

Such determinations are generally difficult because the reaction under investigation is usually only a very minor channel of the overall reaction, and the electronically excited product, though easily detected, has a short lifetime. Furthermore, unlike measurements of total rate coefficients under pseudo-first-order conditions, which require knowledge of the concentration of only one reactant, measurements of these absolute partial rate constants require simultaneous determination of the absolute concentrations of both reactants and of the electronically excited product. Thus far, this has proved to be a highly challenging task, leaving significant uncertainties in the value of the determined partial rate constant, even for those chemiluminescence processes that have been addressed by the most direct techniques.

In this work we focus on the characteristic, intense OH($A^2\Sigma^+$) → OH($X^2\Pi$), $\Delta v = 0$, emission at ca. 308 nm of low-pressure C_2H_2/O/H/O_2 atomic flames and of all hydrocarbon flames. The likely source of OH(A) in hydrocarbon flames has been inferred from a number of experiments and, though not definitely established, the reaction of CH with O_2 has long been the prime candidate.[10,11]

$$\text{CH}(X^2\Pi) + \text{O}_2 \rightarrow \text{OH}(A^2\Sigma^+) + \text{CO} \qquad \text{(1d)}$$

The first attempt at a determination of the source(s) of OH(A) in hydrocarbon flames was that of Porter et al.[12] who performed time-resolved measurements of radicals in low-pressure (18 Torr) lean and rich C_2H_2 and CH_4 flames spanning the temperature range 800 to 2000 K. Concentrations of CH in the $^2\Pi$ ground state were obtained from absorption measurements, whereas absolute concentrations of electronically excited OH were obtained from the 1−0 and 0−0 bands of the $^2\Sigma \rightarrow {}^2\Pi$ transition using the appropriate Franck−Condon factors. Stable species were analyzed by either gas chromatography or mass spectrometry. They proposed the CH + O_2 reaction as the mechanism for formation of OH(A) based on the earlier

* Corresponding author.

10.1021/jp035568j CCC: $25.00
Published on Web 11/15/2003

suggestion by Krishnamachari et al.[10] Although correlations of [OH(A)] with [O_2][CH] were not at all obvious from the two flame profiles given, the authors were able to give an order-of-magnitude estimate of the rate constant (800 to 2000 K) as 1×10^{-13} cm^{-3} s^{-1}. In another study of the same period, spectroscopic analyses of C_2H_2 flames by Becker et al.[13] showed that OH(A) is formed rotationally hot and that the related emission intensity scales with [O_2]. From this observation, and by elimination of several other candidate reactions for OH(A) formation on energetic grounds, the reaction CH + O_2 was also proposed as the most likely OH(A) source.

In a later study, Grebe and Homann[1] used a flow reactor in which emission of OH(A) from a C_2H_2/O/H reaction system at room temperature and at ca. 2 Torr was analyzed. Absolute concentrations of OH(A) were obtained by calibrating the optical system using the known radiation intensity from the reaction O + NO → NO_2^* and a calibrated tungsten ribbon lamp. In the absence of O_2 these authors observed a small OH(A) emission which they attributed to O_2 contamination, arising probably from O recombination. An underlying quasi-continuum emission was also observed, similar to that found earlier by Fontijn.[14] Their results showed that [OH(A)] increased linearly with [O_2] as long as $[O_2]_0$ was less than $[C_2H_2]_0$. As $[O_2]_0$ became larger than $[C_2H_2]_0$, the increase in OH(A) per O_2 became smaller and then leveled off or passed a maximum. [OH(A)] was also found to be proportional to [O] when [C_2H_2] and [O_2] were fixed. Concentrations of CH were however not measured in these experiments, but calculated based on an assumed reaction mechanism for production and consumption of CH. Thus, accepting the reaction CH + O_2 as a source of OH(A), they estimated the rate constant of k_{1d} from the measured [OH(A)] profiles and the calculated [CH] profiles: $k_{1d} = 8 \times 10^{-14}$ cm^{-3} s^{-1} at room temperature. This value is similar to that, at higher temperatures, estimated by Porter et al.[12] However, as mentioned by the authors, there were still some inconsistencies for mixtures with high initial $[O]_0$ or $[O_2]_0$ relative to $[C_2H_2]_0$.

The latest study on OH(A) chemiluminescence in hydrocarbon flames is that of Smith et al.,[15] who derived a rate constant for the OH(A)-forming channel of 3×10^{-13} cm^{-3} s^{-1} in the range 1500 to 1950 K, somewhat higher than that at room temperature by Grebe and Homann,[1] suggesting an activation energy of ca. 4 kJ mol^{-1}. Smith et al.[15] derived this value by comparing the measured absolute OH(A) concentrations in the central flow of a series of lean-to-rich methane−air flames with that predicted by a detailed chemical model. Absolute concentrations of OH(A) in the central flow region were determined by calibration of the optical detection system using Rayleigh scattering in N_2 and by Abel inversions on the line-of-sight emission data.

In kinetic studies of the elementary CH + O_2 reaction, Messing et al.[16] and Bergeat et al.,[17] using appropriate sources of CH radicals, established directly that this reaction does indeed produce OH(A) as a minor primary product. In these studies, the total rate constant of the CH + O_2 reaction was derived to be $k_1 = (3.3 \pm 0.4) \times 10^{-11}$ cm^3 s^{-1} and $(3.6 \pm 0.5) \times 10^{-11}$ cm^3 s^{-1}, respectively.

In addition to the channel producing electronically excited OH radicals, many other reaction channels are available from the highly exoergic CH + O_2 reaction, including formation of other excited species.

$$\mathrm{CH}(\mathrm{X}^2\Pi) + \mathrm{O}_2\,(\mathrm{X}^3\Sigma_g^-) \rightarrow \mathrm{CO}_2 + \mathrm{H} \qquad \Delta_r H_{298}^\circ = -774\ \mathrm{kJmol}^{-1} \quad (1a)$$

$$\rightarrow \mathrm{OH} + \mathrm{CO} \qquad \Delta_r H_{298}^\circ = -668\ \mathrm{kJmol}^{-1} \quad (1b)$$

$$\rightarrow \mathrm{O} + \mathrm{HCO} \qquad \Delta_r H_{298}^\circ = -305\ \mathrm{kJmol}^{-1} \quad (1c)$$

$$\rightarrow \mathrm{OH}(\mathrm{A}^2\Sigma) + \mathrm{CO} \qquad \Delta_r H_{298}^\circ = -277\ \mathrm{kJmol}^{-1} \quad (1d)$$

$$\rightarrow \mathrm{O} + \mathrm{H} + \mathrm{CO} \qquad \Delta_r H_{298}^\circ = -240\ \mathrm{kJmol}^{-1} \quad (1e)$$

$$\rightarrow \mathrm{O}(^1\mathrm{D}) + \mathrm{HCO} \qquad \Delta_r H_{298}^\circ = -116\ \mathrm{kJmol}^{-1} \quad (1f)$$

$$\rightarrow \mathrm{OH} + \mathrm{CO}(\mathrm{a}^3\Pi) \qquad \Delta_r H_{298}^\circ = -81\ \mathrm{kJmol}^{-1} \quad (1g)$$

$$\rightarrow \mathrm{O}(^1\mathrm{D}) + \mathrm{H} + \mathrm{CO} \qquad \Delta_r H_{298}^\circ = -50\ \mathrm{kJmol}^{-1} \quad (1h)$$

where the enthalpies of reaction were calculated using data from references 18 and 19.

To establish that the above reaction is indeed the source of OH(A) in low-pressure C_2H_2/O/H/O_2 flames, we have applied a quasi-steady-state method, similar to that used in a previous study by this group,[5] of the chemiluminescence reaction C_2H + O(^{3}P) → CH($A^2\Delta$) + CO. We have also determined the rate constant for the title reaction at room temperature and estimated its temperature dependence from several other experiments at higher temperatures.

2. Experimental Section

a. Experimental Setup. All measurements were carried out using a conventional discharge-flow/molecular beam sampling−threshold ionization mass-spectrometry (D−F/MB-TIMS) apparatus, which has been described on several earlier occasions.[20,21] The main features pertinent to the present experiments are given here.

The flow reactor consists of a cylindrical quartz tube (i.d. = 16.5 mm) equipped with a discharge sidearm, an axially movable central injector tube, and an additional side inlet to admit carrier gas. Acetylene, diluted in helium, was added through a central injector tube. Oxygen and hydrogen atoms were generated by a 75 W microwave discharge through O_2/H_2/He mixtures. The reactor wall was treated with 10% HF solution to suppress loss of radicals at its surface.

Following mixing of the C_2H_2/He and O/H/He flows, CH radicals are rapidly produced via two chemical paths,[22−25] both initiated by the oxidation of C_2H_2:

$$\mathrm{C_2H_2} + \mathrm{O} \rightarrow \mathrm{HCCO} + \mathrm{H} \quad (2a)$$

$$\rightarrow {}^3\mathrm{CH_2} + \mathrm{CO} \quad (2b)$$

$$\mathrm{HCCO} + \mathrm{H} \rightarrow {}^1\mathrm{CH_2} + \mathrm{CO} \quad (3)$$

$${}^1\mathrm{CH_2} + \mathrm{M} \rightarrow {}^3\mathrm{CH_2} \quad (4)$$

$${}^3\mathrm{CH_2} + \mathrm{H} \rightarrow \mathrm{CH} + \mathrm{H_2} \quad (5)$$

The CH is removed by fast reactions, mainly with O, H, C_2H_2, and O_2.[22−24] The CH concentration then changes gradually along the flow as its chemical precursors are consumed. The average lifetime of CH in our experiments is only ca. 20 μs, which is very short compared to the reaction times. As a result, [CH] is always very close to quasi-steady steady.

Quantitative and qualitative analyses of the relevant species in the investigated C_2H_2/O/H atomic flames were achieved using MB-TIMS. The core of the gas flow at the reactor exit was sampled by a 0.3 mm-diameter pinhole in a quartz cone giving access to the first of two differentially pumped low-pressure chambers. After mechanical modulation to allow phase-sensitive detection, the resulting molecular beam enters the second low-pressure chamber, which houses the electron impact ionizer and an extranuclear quadrupole mass spectrometer. A lock-in amplifier was used to distinguish between beam and background ions.

Concentrations of the primary reactants C_2H_2, O, and H were recorded at electron energies only a few electronvolts (eV) above the respective ionization potentials in order to suppress signal contamination by fragment ions. O_2 was ionized at an electron energy of 70 eV. The CH radicals were monitored at a nominal electron energy of 10.6 eV.

Absolute concentrations of the molecules C_2H_2, O_2, H_2, and NO (used in additional experiments) were derived from measured fractional flows of certified high-purity gases and from total pressure. The instrumental sensitivities toward the absolute concentrations of O and H atoms were determined by partial dissociation of O_2 and H_2, respectively, in a microwave discharge and application of the discharge on/off method.[20] Typical initial concentrations of the reactants were as follows: $[C_2H_2]_0 \approx$ (1 to 3) $\times 10^{14}$ cm^{-3}, $[O]_0 \approx$ (1 to 4) $\times 10^{14}$ cm^{-3}, $[H]_0 \approx$ (1 to 4) $\times 10^{14}$ cm^{-3}, $[O_2]_0 =$ (0.3 to 17) $\times 10^{14}$ cm^{-3}.

Electronically excited OH radicals, OH($A^2\Sigma^+$), were detected at a fixed point, 2.5 cm upstream of the MS sampling cone, by radiative emission that passed through an optical port and was imaged by a quartz lens through an Oriel narrow-band-pass filter (308 ± 6 nm) onto a Hamamatsu 1P28 photomultiplier tube (PMT). Thus, to correlate the OH(A) emission intensity to species concentrations obtained by MS, the flow injector position (defining the point of initiation of the C_2H_2/O/H flame) was duly adjusted by 2.5 cm between intensity measurements and MS measurements such that the reaction times (and hence the reaction history) for both were identical.

All experiments were carried out at a total pressure of 2 Torr (He). In addition to measurements carried out at room temperature, several experiments were performed at higher flow reactor (nominal) temperatures of 450, 620, and 930 K, though the temperature of the gas at the sampling points for CH and OH(A) were much lower (see below). Several linear gas flow velocities through the reactor were used: 19, 39, 44, 49, and 54 m s^{-1}, the first two corresponding to a temperature of 296 K and the latter three to reactor temperatures at the OH(A) detection points of 355, 420, and 511 K, respectively. For some experiments, reaction times were altered between ca. 2 ms to ca. 13 ms by changing the injector position. However, during most experiments $[O_2]_0$ was varied and the reaction time fixed. Pure gases and mixtures were used without further purification: He (99.9996%) as discharge in-let carrier gas, and certified mixtures: 5.0% C_2H_2 (99.96% pure), 10.0% O_2 (99.998% pure), 5.07% H_2 (99.999% pure), and a 10.0% mixture of NO (99.999%) all with 99.999% pure He (UCAR).

b. Methodology. Identification of reaction 1d as the main source of electronically excited OH relies upon the short lifetime of OH(A) ($\tau_{\text{radiative}} = 0.8$ μs) compared to the overall reaction time (of several ms), such that OH(A) has a quasi-steady-state concentration. Under such conditions, and provided that OH(A) is produced only by reaction 1d, the [OH(A)] should always be proportional to the product $[CH][O_2]$ in all possible reaction conditions:

$$[OH(A)]_{ss} = \frac{k_{1d}[CH][O_2]}{\sum_y (k_{qy}[Q_y]) + k_{q(O_2)}[O_2] + A_{nm}} \qquad \text{(i)}$$

where k_{qy} is the quenching rate constant of OH(A) by species Q_y and A_{nm} is the Einstein coefficient for spontaneous emission [OH(A) → OH(X)]. The denominator of eq i remained approximately constant under our experimental conditions since the sum of the quenching rates[26−28] remained always about a factor of 7 smaller than the emission rate. Further, of the main quenching species He, C_2H_2, and O_2, only the latter was varied during some measurement sets; this variation resulted in a change in the denominator of less than 7%. This change was however taken into account by applying the necessary multiplication factor to the observed emission intensity, shown below. Under our experimental conditions and at room temperature the OH(A) quenching rates used to determine the value of the denominator were $k_{qC_2H_2} = 3.3 \times 10^{-10}$ cm^3 s^{-1} (ref 29), $k_{qO_2} = 8 \times 10^{-11}$ cm^3 s^{-1} (ref 29), and $k_{qHe} = 2 \times 10^{-13}$ cm^3 s^{-1} (ref 30).

Thus, eq i may be reformulated in terms of intensity, I_{obs}, impinging on the photocathode.

$$I_{obs} = BA_{nm}[OH(A)] = B\Phi k_{1d}[CH][O_2] \qquad \text{(iia)}$$

where

$$\Phi = \frac{A_{nm}}{A_{nm} + \sum_y (k_{qy}[Q_y]) + k_{qO_2}[O_2]} \qquad \text{(iib)}$$

is the OH(A) emission quantum yield, while B is a catch-all constant expressing the overall sensitivity of the optical/detection system. As mentioned above, Φ varied slightly over the course of some measurement sets due to changes in $[O_2]$. For example, for the room-temperature measurements Φ ranged from 0.88 to 0.93.

Thus, if reaction 1d is the sole source of OH(A) in the reaction system investigated, all plots of I_{obs}/Φ vs $[CH][O_2]$ will be linear and pass directly through the origin. Note that only relative intensities and relative concentrations need be known to demonstrate this. If the measured intensities can be related to [OH(A)] and if the absolute concentrations of [CH] (and $[O_2]$) are determined, the rate constant k_{1d} can be found directly from the gradient of the I_{obs}/Φ vs $[CH][O_2]$ plot.

To test this hypothesis it is desirable to cover the widest possible range of the product $[CH][O_2]$ and also perform measurements under several different conditions (i.e., initial concentrations of the input reactants, C_2H_2, O, H, and O_2, reaction time, and reactor temperature).

As $[O_2]$ remained quasi-constant over the reaction time, two different approaches were employed to obtain the widest possible range of the product $[O_2][CH]$. The first method was to fix all input reactant flows and measure the relevant relative concentrations and emission intensity at several reaction times by adjusting the position of the central injector tube. The second

was to fix the reaction time (i.e., the central injector tube position) and all flows except that of O_2/He and He, so that $[O_2]_0$ could be varied over a wide range (ca. a factor of 30 for some measurements) while maintaining a constant total reactor pressure. Over this large $[O_2]$ range the relative [CH] changed by only a factor of about three.

The temperature of the $C_2H_2/O/H/O_2$ system was also elevated for three sets of measurements by means of a resistively heated jacket that surrounded the flow tube up to 3 cm before the MS sampling cone. These high-temperature measurements primarily served to extend the range of reaction conditions (temperature and, particularly, chemical composition) under which OH(A) and CH were monitored. However, since the heating jacket did not extend to the detection regions, a temperature gradient existed beginning 5 cm before the MS sampling cone. This meant that the actual temperature of the gas sampled by the mass spectrometer remained low at 330 ± 20 K[31] for all elevated flow temperatures (those measured at the center of the heating jacket), whereas the temperatures of the OH(A) sampling point were 511 ± 15, 420 ± 10, and 355 ± 10 K for nominal reactor temperatures of 930, 620, and 450 K, respectively.

Even though the temperatures of the two sampling points (for OH(A) and CH/O_2, respectively) differed in these higher-temperature measurements, correlations between [OH(A)] and $[CH][O_2]$ remain a valid method to verify the dominant source of [CH] under our experimental conditions. Kinetic modeling based on the $C_2H_2/O/H/O_2$ mechanism of Peeters et al.[23,24,32] shows that the ratio of the CH concentrations $[CH]_{em}/[CH]_{MS}$ at the OH(A) emission and MS sampling points for a given temperature difference is constant within $\pm$ 6%, independent of the precise reaction conditions and regardless of $[O_2]_0$ being varied over an order of magnitude. For example, the ratio $[CH]_{em}/[CH]_{MS}$ is calculated to be 3.34 for the experiments at a nominal flow reactor temperature of 920 K with initial concentrations $[H]_0 = 3.0 \times 10^{13}$ cm^{-3}, $[O]_0 = 5.6 \times 10^{13}$ cm^{-3}, $[C_2H_2]_0 = 7.5 \times 10^{13}$ cm^{-3}, and $[O_2]_0 = 1.4 \times 10^{15}$ cm^{-3}. An order-of-magnitude variation of $[O_2]_0$, from 2.8×10^{14} cm^{-3} to 2.8×10^{15} cm^{-3} changes the calculated ratio $[CH]_{em}/[CH]_{MS}$ from 3.54 to 3.15. Variation separately of $[C_2H_2]_0$ or $[O]_0$ by a factor of 3 caused negligible change in the calculated ratio. For a similar variation in $[H]_0$, a change of 3% was calculated. The effective activation energy for the (steady-state) CH concentration appears to be 9.4 kJ mol^{-1}, which can be largely attributed to the activation energy of 13 kJ mol^{-1} of the controlling primary step, $C_2H_2 + O$,[33] which is decreased by the slightly negative *T*-dependences of two intermediate steps in the mechanism, i.e., collisional quenching of singlet CH_2 to the triplet[34,35] and the reaction of triplet CH_2 with H to form CH.[36]

3. Results and Discussion

To ascertain first that the observed chemiluminescence of the investigated $C_2H_2/O/H/O_2$ atomic flames can be fully assigned to OH(A $\rightarrow$ X) transitions, several low-resolution (fwhh of 2.0 nm) spectra of the emission were recorded. Though transitions from individual rotational levels were not resolved, our spectrum shows the broad characteristics of the higher resolution chemiluminescence spectra obtained by Becker et al.[13] and Bergeat et al.,[17] both of which show OH(A) to possess a 'hot' rotational and vibrational distribution. In their study of the isolated CH + O_2 reaction, using $CHBr_3$ + K as a clean CH source, Bergeat et al.[17] performed a more detailed spectral analysis of the OH(A$-$X) emission, showing the vibrational population ratio of the A state to be $P(v' = 1)/P(v' = 0) = 0.46$ and $v' = 0$ and $v' = 1$ to be formed with very different rotational population distributions. Neither rotational distribution was found to be Boltzmann; however, the best fit to a Boltzmann distribution for $v' = 0$ corresponded to $T = 14\,000$ K and that for $v' = 1$ to $T = 4400$ K. For comparison with our experimental spectrum, the solid line of Figure 1, two simulated[37] spectra are displayed; one with the vibrational population and Boltzmann rotational distributions given by Bergeat et al.[17] (dashed line), the other for 300 K Boltzmann vibrational and rotational distributions (dotted line), all at a resolution of 2 nm. It is clear that our experimental spectrum shows OH(A) to be formed with vibrational and rotational population distributions nearly identical to those observed by Bergeat et al.[17] This is expected if the source of OH(A) is the same reaction, viz. reaction 1d, in both cases given that in both studies vibrational and rotational energy transfer rates are expected to be low compared to the rate of spontaneous emission.[17,38,39]

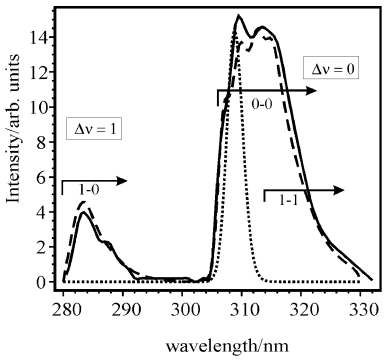

Figure 1. OH(A$\rightarrow$X) emission spectrum at 2 nm resolution. The solid line is the observed emission from our $C_2H_2/O/H/O_2$ reaction system at 296 K, the dashed line is a simulated emission spectrum using the 'hot' Boltzmann vibrational and rotation population distribution for OH(A) derived by Bergeat et al.,[17] and the dotted line is a simulated emission spectrum with OH(A) possessing a rotational and vibrational Boltzmann distribution corresponding to room temperature.

We can also conclude from our OH emission spectrum that interference from formation, in the microwave discharge, of any metastable oxygen, $O_2(^1\Delta)$, is negligible. This is because any OH(A) formed in a reaction between CH(X) and $O_2(^1\Delta)$ is expected to possess a rotational and vibrational distribution that is very different than that for the distribution produced by the $CH(X) + O_2(X^3\Sigma_g^-)$ reaction given the 94 kJ mol^{-1} extra energy in the former process. Note that no $O_2(^1\Delta)$ was present in the experiments of Bergeat et al.[17] since in that study CH was produced by reaction of potassuim with bromoform. There is also expected to be little interference from reactions of vibrationally hot CH with O_2 since the main formation reaction of CH in our system, $CH_2 + H \rightarrow CH + H_2$, is exothermal by only 14 kJ mol^{-1}, which is less than the $v'' = 1$ to $v'' = 0$ energy gap of 34 kJ mol^{-1}.

For all our I_{obs} measurements, the baseline (zero) value was taken as that observed under normal experimental flow conditions with the microwave discharge operating but in the absence of C_2H_2. Under these conditions no spectral features corresponding to OH(A $\rightarrow$ X) emission could be detected.

a. Linear Relation between I_{obs}/Φ and $[CH]_{rel}[O_2]_{rel}$. Our main objective was to verify whether the reaction 1d, $CH(X^2\Pi) + O_2 \rightarrow OH(A^2\Sigma) + CO$, is indeed the dominant source of $OH(A^2\Sigma)$ under all reaction conditions. To this end, two series of measurements were taken at 296 K: one set in which the injector position was altered in order to change the reaction time at the measurement points, the second in which the reaction

TABLE 1: Experimental Conditions for the Two Series of Measurements Carried Out on the $C_2H_2/O/H/O_2$ Reaction System at 296 K

flow velocity (cm s^{-1})	injector-to-sampling distance (cm)	$[C_2H_2]_0$ (cm^{-3})	$[O_2]_0$ (cm^{-3})	$[H]_0$ (cm^{-3})	$[O]_0$ (cm^{-3})
1907	4 to 24	3.54×10^{14}	4.46×10^{14}	5.29×10^{14}	4.19×10^{14}
3387	20	2.05×10^{14}	3.3×10^{13} to 9.6×10^{14}	3.61×10^{14}	2.80×10^{14}

time was fixed and the O_2 flow was changed. Table 1 gives a summary of the conditions under which the 296 K measurements were taken.

Figure 2 shows the results of the two series of measurements described above. The observed emission intensity for the last set of measurements changed by 2 orders of magnitude. The solid line represents the best least-squares linear fit through the data points, allowing both the gradient and the intercept to vary freely. For this fit the correlation coefficient is 0.997 and there is a very small *y*-axis intercept of 1.0 ± 0.2. The intercept can be seen more clearly in the inset plot, which shows the lower value data points in more detail. The dashed line represents the best least-squares linear fit through all data points which is forced through the origin and therefore has the form of eq iia; here the correlation coefficient is 0.994. The excellent correlation coefficient shows unambiguously that reaction 1d is indeed the dominant OH(A) source in the $C_2H_2/O/H/O_2$ systems. The very small intercept of the solid line could indicate a minor contribution to OH(A) formation from a source other than reaction 1d; however, the intercept may also be a result of small systematic errors incurred by slight intensity changes in the glow from the microwave discharge region.

As outlined above, to achieve as wide a range of reaction conditions as possible, a series of measurements on the $C_2H_2/O/H/O_2$ reaction system were carried out with the flow reactor heated to temperatures of 450, 620, and 930 K. These values represent the temperature of the gas at all flow distances except in the region 0 cm to 5 cm from the MS cone where a temperature gradient existed. As explained in the previous section, this temperature gradient resulted in a lower gas temperature at the OH(A) monitoring point of 355, 420, and 511 K for the main flow temperatures of 450, 620, and 930 K, respectively, and in temperatures at the CH sampling point of $330 \text{ K} \pm 20$ K for each of these cases.

For these measurements, the reaction time was fixed and $[O_2]$ was varied as this procedure gave a wider range in OH(A) concentration at the emission sampling point. As with the measurements at room temperature, variation of $[O_2]$ also produced a change in [CH] at the MS sampling point.

These higher-temperature results are displayed in Figure 3. Each set of data has been arbitrarily scaled for clarity. Again the straight lines through the data points represent least-squares fits. The solid line ($f(x) = mx + c$) through the 420 K data is omitted as it is indistinguishable from the fit forced through zero (dashed line). As with the data obtained at 296 K, it is clear from these plots that the correlation between I_{obs} and $[CH][O_2]$ is excellent and that intercepts are negligible, showing that the title reaction is by far the dominant, if not the only, source of OH(A) in these low-pressure $C_2H_2/O/H/O_2$ atomic flames.

Based both on its ionization potential close to that of CH($X^2\Pi$) and relationship to the $C_2H_2/O/H$ reaction system, the metastable electronically excited species CH($a^4\Sigma^-$) could have an influence on our observations if reaction 6a is sufficiently rapid

$$CH(a^4\Sigma^-) + O_2 \rightarrow OH(A^2\Sigma^+) + CO \quad (6a)$$

$$\rightarrow \text{other products} \quad (6b)$$

CH($a^4\Sigma^-$) has been detected in C_2H_2/O reaction systems[40] and has been postulated to be formed by reaction 1 followed by (7a)[32]

$$HCCO + O \rightarrow CH(a^4\Sigma^-) + CO_2 \quad (7a)$$

$$\rightarrow \text{other products} \quad (7b)$$

Reaction 5, the known dominant source of CH(X) in $C_2H_2/O/H/O_2$ flames, does not form CH($a^4\Sigma^-$).[32] There could be two routes to the interference of reaction 6a to our measurements. First, a significant portion of the detected CH signal could be

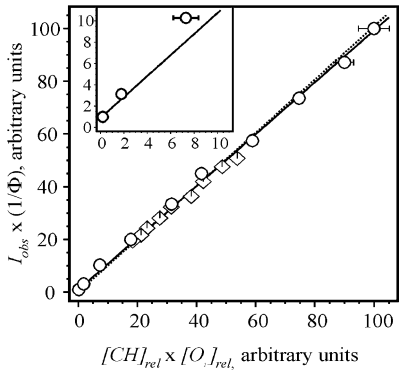

Figure 2. Correlation between relative OH emission intensity and the relative concentration product $[O_2][CH]$ for the $C_2H_2/O/H/O_2$ reaction system at 296 K and 2 Torr. The filled circles are data taken at a fixed reaction time with systematic variation of $[O_2]_0$. The open squares are data taken at several different reaction times while keeping all flow rates fixed. The inset plot shows the lowest data points in more detail. The solid line represents the best least-squares linear fit through the data points. The dashed line is a least-squares linear fit forced through the origin.

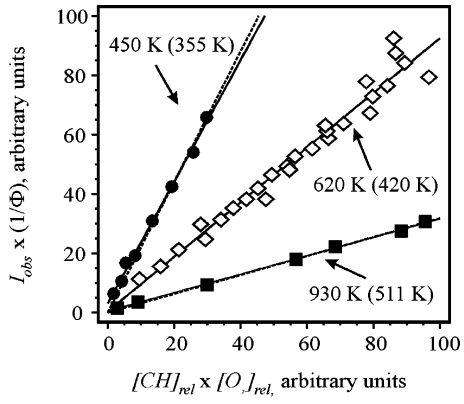

Figure 3. Correlation between relative OH emission intensity and the relative concentration product $[O_2][CH]$ for the $C_2H_2/O/H/O_2$ reaction system at three elevated temperatures. The data are a result of measurements taken at a fixed reaction time with systematic variation of $[O_2]_0$. The temperature indicated for each set of data is the nominal temperature of the flow, whereas the associated temperature at the point of OH emission is enclosed in brackets. The solid lines represents the best least-squares linear fit through the data points. The dashed lines are least-squares linear fits forced through the origin. Each data set has been arbitrarily scaled for clarity.

due to $CH(a^4\Sigma^-)$ since its ionization potential lies 0.74 eV below that of CH(X).[41] Second, reaction 6a could still be partly responsible for production of OH(A) if k_{6a} is sufficiently high, though this requires that the contribution of $CH(^4\Sigma^-)$ to the CH MS signal remains constant given the linear relationships of Figures 2 and 3.

The first concern is easily dismissed. Taking the rate constant value from Peeters et al.[42] for the CH-producing channel of HCCO + O and assuming all CH is $CH(a^4\Sigma^-)$, then the quasi-steady-state concentration of $CH(a^4\Sigma^-)$ is modeled to be only in the low 10^8 cm^{-3} range, which is much below the modeled and measured [CH(X)] of around 10^{10} cm^{-3}. Actually, in our experimental conditions the predicted $CH(a^4\Sigma^-)$ concentration is below our detection sensitivity at the ionizing electron energy used for CH detection.

The second concern hinges on the constancy of the CH(X)/$CH(a^4\Sigma^-)$ ratio. Based on the main formation reactions of CH(X) and $CH(a^4\Sigma^-)$, reactions 2−5 for CH(X) and reaction 2a followed by reaction 7a for $CH(a^4\Sigma^-)$, it is expected that their temporal profiles will be very different in our reaction systems. The formation of the metastable state has a strong dependence on the O-atom concentration, which decreases along the flow. On the other hand, initial H-atom concentrations are approximately maintained, or decrease only slightly, along the flow. Our kinetic model of the 296 K system shows that over the reaction time from 2 to 12 ms, [CH(X)] should change by a factor of about 2.4 (a factor of 2.8 is measured), whereas [$(CH(a^4\Sigma^-)$] should change by a factor of 10. Should $CH(a^4\Sigma^-)$ + O_2 contribute to OH(A) formation signal, the two correlations shown in Figure 2 should differ markedly since one is taken as a function of reaction time, with [CH(X)]/[$CH(a^4\Sigma^-)$] expected to vary strongly, while the other is taken at a fixed reaction time but as a function of [O_2] with [CH(X)]/[$CH(a^4\Sigma^-)$] expected to remain approximately constant.

A negligible propensity for $CH(a^4\Sigma^-) + O_2(X^3\Sigma_g^-)$ to form OH + CO can be expected a priori, as this interaction is most likely to proceed via a twin σ combination forming a highly activated cyclic $H[\dot{C}(O)O]^\dagger$ intermediate that promptly decomposes to H + CO_2.

b. Absolute Determination of k_{1d}. Having established that CH + O_2 is the only significant source of OH(A) in our low-pressure C_2H_2/O/H/O_2 reaction system, we now turn our attention to determining the rate constant k_{1d}. Equation iia shows that determination of k_{1d} relies on evaluation both of B and [CH].

The determination of [CH] is straightforward. We assume that the sensitivity of the MB-TIMS apparatus for CH, S_{CH}, is half that of $S_{C_2H_2}$ at identical excess ionizing electron energy above the respective ionization potentials and under the same experimental conditions. The adopted factor 0.5 takes into consideration the reduced collision cross-section of CH compared to C_2H_2. The expected uncertainty for this widely applied "additivity of atomic cross-sections" procedure is about a factor of 2.[43]

The recorded voltage associated with the collected OH(A) chemiluminescence signal, I_{obs}, can be converted to photon emission rate, E(OH*), on the basis of the measured signal, I(NO_2*), for the well characterized chemiluminescence sequence of reactions of NO with O[44,45]

$$NO + O \rightarrow NO_2 + h\nu \qquad (6a)$$

$$NO + O + M \rightarrow NO_2^* + M \rightarrow NO_2 + M + h\nu \qquad (6b)$$

This reference reaction is ideally suited as a quantitative standard because (i) it appears as a continuous spectrum from 400 to 1400 nm and (ii) the emission rate is independent of the total pressure in the 0.5 Torr to 10 Torr range and is directly proportional to the concentration product [NO][O], which is easy to determine. Fontijn et al.[44] determined the absolute total rate constant k_6 at room temperature:

$$k_6 = (6.4 \pm 1.9) \times 10^{-17}\ cm^3\ s^{-1}$$

We can write

$$E(OH^*) = I(OH^*)\frac{E(NO_2^*)B_{NO_2^*}}{I(NO_2^*)B_{OH^*}} \qquad (iii)$$

with the photon emission rate $E(NO_2^*)$ given by the known product k_6[NO][O]. The respective $B_{i^*} \equiv I_{i^*}/E_{i^*}$ are found from the measured or known spectral distributions of the emissions $E_n(\lambda)$, convoluted by the transmission curves $Tr_f(\lambda)$ of the respective filters and the spectral response $R(\lambda)$ of the PMT:

$$\frac{I_i^*}{E_i^*} = \frac{g\int E_n(\lambda)Tr_f(\lambda)R(\lambda)\,d\lambda}{\int E_n(\lambda)\,d\lambda} \qquad (iv)$$

Since one needs only the ratio B_{NO_2}/B_{OH^*} and since the two measurements were carried out in exactly identical conditions the geometrical photon collection factor g cancels.

The $I(NO_2^*)$ reference emission intensities and the corresponding [NO] and [O] were monitored in an NO/O mixture diluted in He, with O atoms also created by partial dissociation of O_2, under exactly the same experimental conditions.

The resulting k_{1d} value at 296 K is

$$k_{1d}(296\ K) = 8.0_{-5}^{+10} \times 10^{-14}\ cm^3\ s^{-1} \qquad (v)$$

The error range given for the determined rate constant is estimated based on possible systematic errors associated with calibration of [CH] (viz. the instrument sensitivity) and of [OH(A)] (with a large part of this uncertainty due to the uncertainty of the published rate constant k_6). As can be seen from the presented data, random errors in the measurements were very small by comparison. This value of k_{1d} at 296 K agrees with that reported by Porter et al.[12] and by Grebe and Homann,[1] although the close agreement with the latter is fortuitous given that their [CH] was calculated using an outdated kinetic model. Taken together, these three investigations point toward an only weak temperature dependence for k_{1d}. With both [CH] and OH(A) emission rate calibration factors determined, the data for all temperatures (at the OH(A) sampling point) may be compared. Figure 4 shows correlations between absolute values of $[CH]_{330K}[O_2]_{Te}$ and absolute OH(A) emission rates. Here the subscripts represent the temperatures at which the concentrations were determined, with the exception of the room-temperature measurements when all concentrations relate to 296 K. The temperature T_e at which OH(A) emission rates were measured and [O_2] is represented is given in the figure. Values of $[O_2]_{Te}$, at the OH(A)-emission sampling point, were related to those measured at the CH sampling point, $[O_2]_{330K}$, by muliplication of the latter by 330/T. The slopes of these plots are 7.97×10^{-14} cm^{-3} s^{-1} for 296 K, 1.07×10^{-13} cm^{-3} s^{-1} for $T_e = 355$ K, 1.86×10^{-13} cm^{-3} s^{-1} for $T_e = 420$ K, and 2.97×10^{-13} cm^{-3} s^{-1} for $T_e = 511$ K. To derive k_{1d} for the measurements on the higher temperature systems, a factor corresponding to $[CH]_{Te}/[CH]_{330K}$ must be applied, as explained in the previous section. These factors are 1.27, 2.08, and 3.34, giving rise to

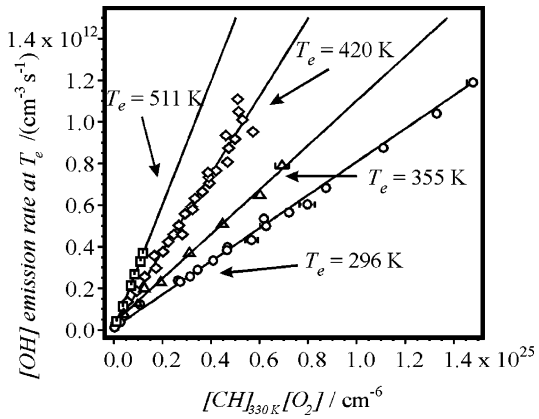

Figure 4. Correlation between absolute OH emission rate and the absolute concentration product $[O_2][CH]$ for the $C_2H_2/O/H/O_2$ reaction system at room temperature and three elevated temperatures. The rate constant k_{1d} for the room-temperature measurements is obtained directly from the gradient of that data set. In this case $[CH]_{330K}$ of the *y*-axis is in fact $[CH]_{296K}$. Rate constants for higher temperatures can also be obtained from the gradients after application of the factors relating $[CH]_{330K}$ to $[CH]_{Te}$ (see text). The solid lines represents the best least-squares linear fit through the data points.

k_{1d} values of 8.4×10^{-14} cm^{-3} s^{-1}, 8.9×10^{-14} cm^{-3}, and 8.9×10^{-14} cm^{-3} s^{-1} at temperatures of T_e of 355, 420, and 511 K, respectively. Thus, from these measurements, for which systematic uncertainties due to calibration of [CH] and [OH(A)] should be very similar to the 296 K measurements, only a weak *T*-dependence (at most) can be seen; our best fit to an Arrhenius expression gives an activation energy of only 0.67 kJ mol^{-1}. Thus, the predicted rate constant at 1700 K (the midrange of the measurements of Smith et al.[15]) is 1.0×10^{-13} cm^3 s^{-1}. The difference between this value and that of Smith et al.[15] is likely attributable to the uncertainties in the absolute values of both determinations (due mainly to calibrations) and not to a large (absolute) uncertainty in the activation energy (as an E_a of 4 kJ mol^{-1} would be required). Our estimates of possible errors give a range for k_{1d} (511 K)/k_{1d}(296 K) of 0.8 to 1.4. The largest value corresponds to an activation energy of 2 kJ mol^{-1}; the maximum we recommend for reaction k_{1d}.

4. Conclusions

We have demonstrated conclusively that the reaction CH + O_2 is responsible for formation of the electronically excited hydroxyl radical in $C_2H_2/O/H/O_2$ atomic flames. We have derived a rate constant for the formation of OH(A) in the CH + O_2 reaction of k_{1d} (296 K) = $8.0^{+10}_{-5} \times 10^{-14}$ cm^3 s^{-1} and further derived an activation energy for this reaction of $0.7^{+1.3}_{-0.7}$ kJ mol^{-1} (296 to 511 K). The general methods described in this work are also applicable to the study of other chemiluminescence reactions and of different flames.

Acknowledgment. S.A.C. gratefully acknowledges support of the Fund for Scientific Research, Flanders (FWO-Vlaanderen), for a postdoctoral mandate and research project (PDM).

References and Notes

(1) Grebe, J.; Homann, K. H. *Ber. Bunsen-Ges. Phys. Chem.* **1981**, *86*, 581.
(2) Grebe, J.; Homann, K. H. *Ber. Bunsen-Ges. Phys. Chem.* **1981**, *86*, 588, and references therein.
(3) Becker, K. H.; Heinemeyer, F.; Horie, O. *Ber. Bunsen-Ges. Phys. Chem.* **1983**, *87*, 898, and references therein.
(4) Dandy, S. D.; Vosen, S. R. *Combust. Sci. Technol*. **1992**, *82*, 131, and references therein.
(5) Devriendt, K.; Peeters, J. *J. Phys. Chem. A* **1997**, *101*, 2546.
(6) Fontijn, A.; Goumri, A.; Brock, P. E. *Combust. Flame* **2000**, *121*, 699, and references therein.
(7) Burke, M. L.; Dimpfl, W. L.; Sheaffer, P. M.; Zittel, P. F.; Bernstein, L. S. *J. Phys. Chem.* **1996**, *100*, 138, and references threrein
(8) Staicu, A.; Stolk, R. L.; Meulen, J. J. *J. Appl. Phys.* **2002**, *91*, 969, and references therein.
(9) Dandy, D. S.; Vosen, S. R. *Combust. Sci. Technol*. **1992**, *82*, 131.
(10) Krishnamachari, S. L. N. G.; Broida H. P. *J. Chem Phys.* **1961**, *34*, 1709.
(11) Gaydon A. G. *The Spectroscopy of Flames*, 2nd ed.; Chapman and Hall: London, 1974.
(12) Porter, R. P.; Clark, A. H.; Kaskan, W. E.; Browne, W. E. *Symp. Int. Combust.* [*Proc.*] **1967**, *11*, 907.
(13) Becker, K. H.; Kley, D.; Norstrom, R. J. *Symp. Int. Combust.* [*Proc.*]-**1969**, *12*, 405.
(14) Fontijn A. *J. Chem. Phys.* **1966**, *44*, 1702.
(15) Smith, G. P.; Luque, J.; Park, C.; Jeffries, J. B.; Crosley, D. R. *Combust. Flame* **2002**, *131*, 59.
(16) Messing, I.; Sadowski, G. M.; Filseth, S. V. *Chem. Phys. Lett*. **1979**, *66*, 95.
(17) Bergeat, A.; Calvo, T.; Caralp, F.; Fillion, J. H.; Dorthe, G.; Loison, J. C. *Faraday Discuss.* **2001**, *119*, 67.
(18) Atkinson, R.; Baulch, D. L.; Cox, R. A.; Hampson, R. F.; Kerr, J. A.; Rossi, M. J.; Troe, J. *J. Phys. Chem. Ref. Data* **1997**, *26*, 521.
(19) Effantin, C.; Michaud, F.; Roux, F.; D'Incan, J.; Verges, J. *J. Mol. Spectrosc*. **1982**, *92*, 349.
(20) Vinckier, C.; Debruyn, W. *Symp. Int. Combust.* [*Proc.*] **1979**, *17*, 623.
(21) Boullart, W.; Devriendt, K.; Borms, R.; Peeters *J. Phys. Chem.* **1996**, *100*, 998.
(22) Boullart, W.; Peeters, J. *J. Phys. Chem*. **1992**, *96*, 9810.
(23) Peeters, J.; Langhans, I.; Boullart, W. *Int. J. Chem. Kinet.* **1994**, *26*, 869.
(24) Peeters, J.; Devriendt, K. *Symp. Int. Combust.* [*Proc.*] **1996**, *26*, 1001.
(25) Devriendt, K.; Van Poppel, M.; Boullart, W.; Peeters, J. *J. Phys. Chem*. **1995**, *99*, 16953.
(26) Fairchild, P. W.; Smith, G. P.; Crosley, D. R. *J. Chem. Phys*. **1983**, *79*, 1795.
(27) Smith, G. P.; Crosley, D. R. *J. Chem. Phys*. **1986**, *85*, 3896.
(28) Wysong, I. J.; Jeffries, J. B.; Crosley, D. R. *J. Chem. Phys*. **1990**, *92*, 5218.
(29) Fairchild, P. W.; Smith, G. P.; Crosley, D. R. *J. Chem. Phys.* **1983**, *79*, 1795.
(30) Assuming a quenching cross-section the same as that of the upper limit measured for Ar [Paul, P. H.; Durant, J. L.; Gray, J. A.; Furlanetto, M. R., *J. Chem. Phys.* **1995**, *102*, 8378].
(31) The temperature of the gas region close to the MS sampling cone was measured using a thermocouple; however, the precise temperature of the gas that is sampled by the cone is more difficult to determine, hence the large uncertainty range quoted here.
(32) Peeters, J.; Boullart, W.; Devriendt, K.; *J. Phys. Chem*. **1995**, *99*, 3583.
(33) Michael, J. V.; Wagner, A. F. *J. Phys. Chem*. **1990**, *94*, 2453, and references therein.
(34) Langford, O. A.; Petek, H.; Moore, C. B. *J. Chem. Phys.* **1983**, *78*, 6650.
(35) Wagner, R. *Z. Naturforsch.* **1990**, *45a*, 649.
(36) Devriendt, K.; Van Poppel, M.; Boullart, W.; Peeters, J. *J. Phys. Chem*. **1995**, *99*, 16953.
(37) Luque, J.; Crosley, D. R. *LIFBASE: Database and Simulation Program (v 1.42)*, SRI International Report MP 98-021, 1998.
(38) Kliner, D. A. V.; Farrow, R. L. *J. Chem. Phys.* **1999**, *110*, 412, and references therein.
(39) Williams, L. R.; Crosley, D. R. *J. Phys. Chem.* **1996**, *100*, 6507, and references therein.
(40) Nelis, T.; Brown, J. M.; Evenson, K. M. *J. Chem. Phys.* **1988**, *88*, 2087.
(41) Kasdan, A.; Herbst, E.; Lineberger, W. C. *Chem. Phys. Lett*. **1975**, *31*, 78.
(42) Peeters, J.; Langhans, I.; Boullart, W.; Nguyen, M. T.; Devriendt, K. *J. Phys. Chem*. **1994**, *98*, 11988.
(43) Peeters, J.; Vinckier C. *Symp. Int. Combust.* [*Proc.*] **1974**, *15*, 969.
(44) Fontijn, A.; Meyer, C. B.; Schiff, H. I. *J. Chem. Phys*. **1964**, *40*, 64.
(45) Becker, K. H.; Groth, W.; Thrain, D. *Chem. Phys. Lett.* **1972**, *15*, 215.